GEOSPATIAL APPROACH FOR URBAN ENVIRONMENTAL QUALITY ASSESSMENT

S. Singh [1,*], K. Jain [1]

[1] Dept. of Civil Engineering, Geomatics group, Indian Institute of Technology Roorkee, Roorkee, Uttarakhand, India
singh14@ce.iitr.ac.in[1]*, kjainfce@iitr.ac.in

Commission III, WG III/7

KEY WORDS: Remote Sensing, Urban Environmental Quality, Urban Greenery, Urban Studies, Principal Component Analysis.

ABSTRACT:

Growing population and change in gentrification patterns of urban areas affect the environment quality, especially in the developing nations. Most cities are thereby, facing serious environmental sustainability challenges. A resilient urban planning is required to solve these environmental problems, which in turn need information that is not available in the desired scales, hence, making it difficult to comprehend. In this study, an approach is proposed to comprehend the environmental quality of a city at community level. Landsat 8 images are used to compute the biophysical indicators, namely, land surface temperature (LST), normalized difference vegetation index (NDVI), normalized difference built-up index (NDBI), modified normalized difference water index (MNDWI) and normalized difference impervious surface index (NDISI) in ArcGIS software. These indicators are then integrated with the indicators from the government census data to compute the community level index for urban environmental quality (UEQI). The results depicted that the highest value of our developed index occurred in the places where there is more of greenery and less built-up area. Based on the obtained UEQI values, different areas of the city are divided into five categories. The index values suggest that urban greening significantly contribute to enhance the urban environmental quality. Also, it highlights the critical zones where intervention should be made by the planners and policymakers for the sustainability of the city.

1. INTRODUCTION

Urbanisation is (Dawson et al., 2017) becoming one of the most significant, inevitable and evident anthropogenic changes altering the earth and life on it. There has been a very high rate of urban growth in the past decades, especially in the developing countries. Urbanization in India accelerated more after independence, due to the mixed economy in the country.

By the end of 2050, most of the population of India will reside in cities, as per the United Nations world's population report (Silva and Clarke, 2002). This will result into considerable amount of land transformations, which in turn will raise environmental concerns like poor resource management, habitat loss, pollutions of land, water and air (Nong and Du, 2011). Increasing growth and employment are a powerful magnet in cities. India's urban population in 2008 was 340 million and is expected to reach 590 million in 2030. The speed of this expansion is quite unlike anything that India has witnessed before. Although growth has attracted investment in urban India, its cities still fail to deliver a basic standard of living to the city dwellers. Achieving a balance between socio-economic development, promoting work opportunities, reducing poverty, and achieving sustainability in societies, continues to stay the largest challenge for the city authorities and urban planners. (Musse, Barona and Santana Rodriguez, 2018). Moreover, urbanisation creates environmental problems due to traffic and associated pollution, pollution due to industries, etc (Cui and Shi, 2012).

Urbanisation without proper planning always has a cost affecting the social and biophysical conditions of the city and ultimately its residents. Diminishing vegetation cover and expansion in impervious surface are the most significant challenges cities face. It affects the hydrological cycle and changes the surface and air temperature which in turn deteriorates environmental health and eventually human health (Chudnovsky, Ben-Dor and Saaroni, 2004). Most Indian cities are facing serious environmental sustainability challenges. Therefore, resilient urban planning is required to solve these environmental problems.

To measure a city's progress towards sustainable development, sets of urban sustainability indicators are formulated by the global and regional organizations (Verma and Raghubanshi, 2018). Since, most of the indicators rely much on census data which is not easily and conveniently available, therefore the capability of remote sensing data is assessed for developing the indicators of environmental quality. Remote sensing has been used widely to monitor changes in urban environment, due to its potential of providing environmental parameters over large spatial and temporal extents (Du et al., 2014).

The urban environmental quality varies in space and time. It is a complex parameter resulting from the interaction between ecological factors, such as the greenness of the city, quality of air and water, geometry and density of buildings, urban heat islands (UHI), etc (Nichol and Wong, 2005). This synthetic index of environmental quality can be formulated from the ecological and environmental data that can in turn be extracted from the satellite imageries (Musse, Barona and Santana Rodriguez, 2018). The information obtained by such composite indices can then be used to detect the changes. Also, to plan actions for environmental remediation.

This study was carried out to develop a method to measure comprehensive environmental quality of Bhopal city. The city is deficient of data about urban environment and also lacks methods to assess it. We saw how remote sensing images can be used to obtain information of the environment at the community/ward level, how the information obtained from remote sensing images be integrated with census data by models, how the city's wards be categorised into different categories of environmental quality, and eventually how the

[1]*Corresponding Author.

https://doi.org/10.5194/isprs-archives-XLIII-B3-2022-705-2022

yielded maps enable monitoring and future planning of development actions.

Environmental variables such as urban greenery, impervious surface and land surface temperature are extracted from Landsat satellite imageries at the city level. In order to assess urban environmental quality, these variables have been integrated with the parameters obtained from census data

2. STUDY AREA AND DATASETS

2.1 Study Area

The study area is the city of Bhopal, the political capital of the central Indian state of Madhya Pradesh, placed at 23.26° N, 77.41° E **Figure 1**. The subtropical climate of Bhopal, ensures hot summers, cool and dry winters, and a humid monsoon. The average temperature of the city is around 25 °C.

The municipal area covers a wide expanse of 463 km^2. The city's population according to 2011 census was around 18 lakhs and as per the ward-wise population data obtained from Bhopal Municipal Corporation (BMC), it reached around 20 lakhs in 2020. For administration purposes, the city is divided into 85 wards, population density and housing density of which are represented in
Figure 2.

The city ranks 16th in size in India and 131st in the world. It is the 20th largest urban agglomeration and one of the 21 fastest growing cities in the world. It is an environmentally sensitive city because of the hills and water bodies. The increased pressure of urbanisation and industrialisation in and around the city has caused an evident and a severe impact on its environmental fabric.

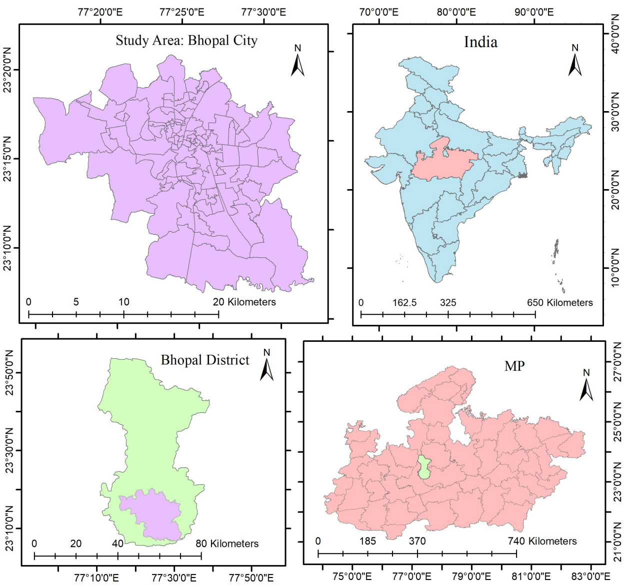

Figure 1. Location of the study area of Bhopal municipal Corporation (BMC).

2.2 Data

To perform the study, Landsat 8, Level 1 images provided by the United States Geological Survey (USGS) for 25th March 2021 are used. The imagery is identified by row 044 and path 145. These satellite images are used to compute the biophysical indicators, namely, LST, NDVI, MNDWI, NDBI and NDISI in ArcGIS software.

The vector map of the city is obtained from the municipal corporation of Bhopal. It is used to find the mean of the physical indicators mentioned above for each ward. Census data such as no of households and population in each ward of Bhopal is also obtained from BMC. The location map of all the slums mushroomed up in different wards of the city, as received from BMC is then digitised and no. of slums in each ward is recorded. A complete database is created.

The ward-wise population and housing densities are represented in **Figure 3.** And the distribution of slums throughout the city is shown in **Figure 4**.

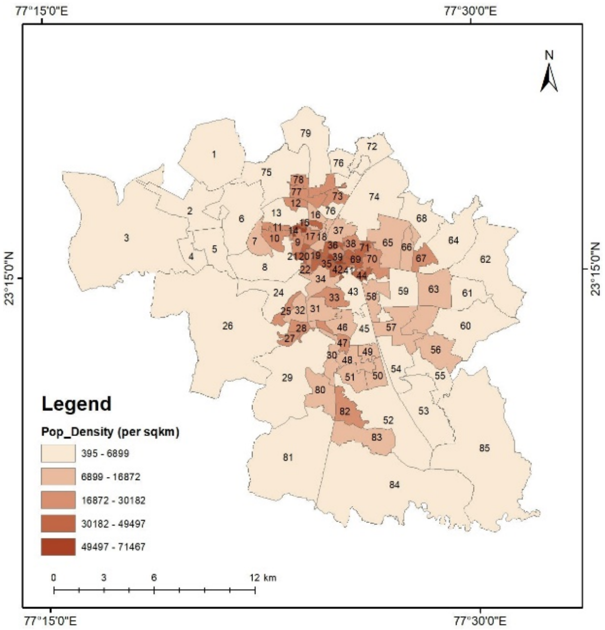

(a)

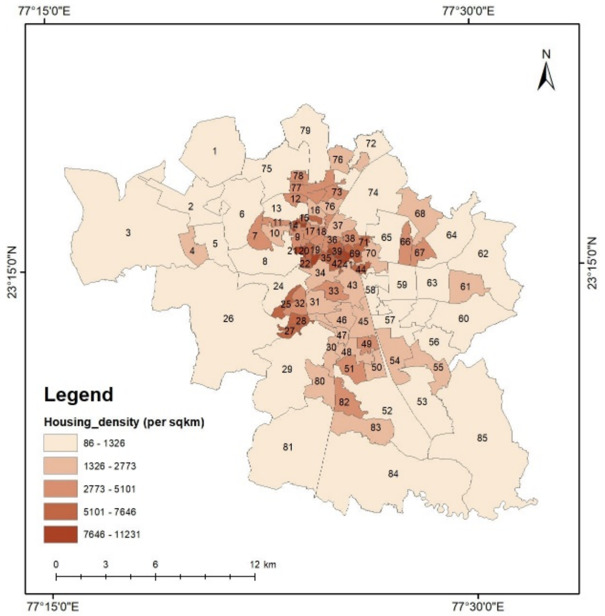

(b)

Figure 2. (a) Population density (PD) map (b) Housing density (HD) map

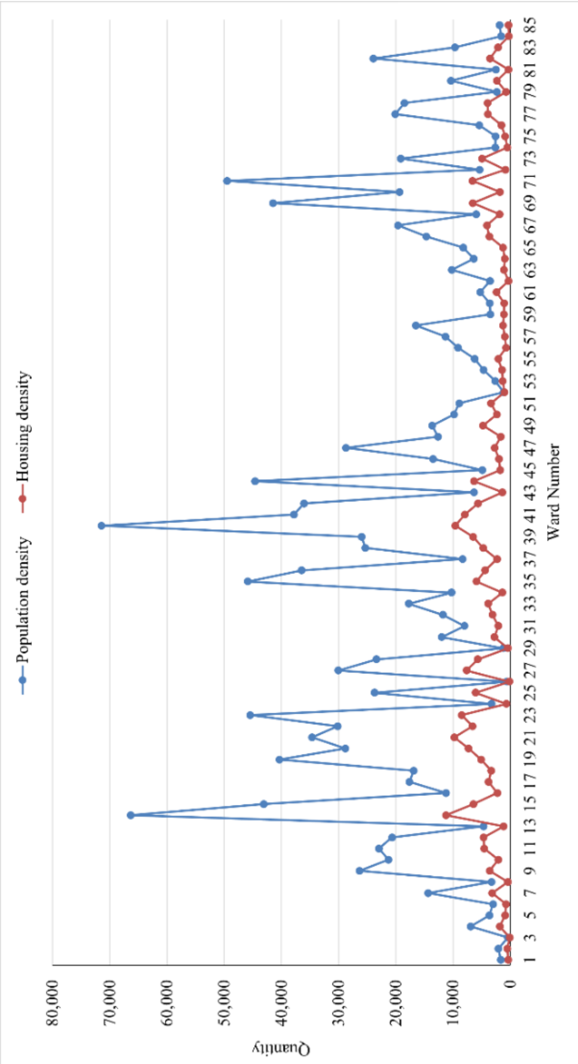

Figure 3. Ward-wise distribution of Population Density and Housing Density

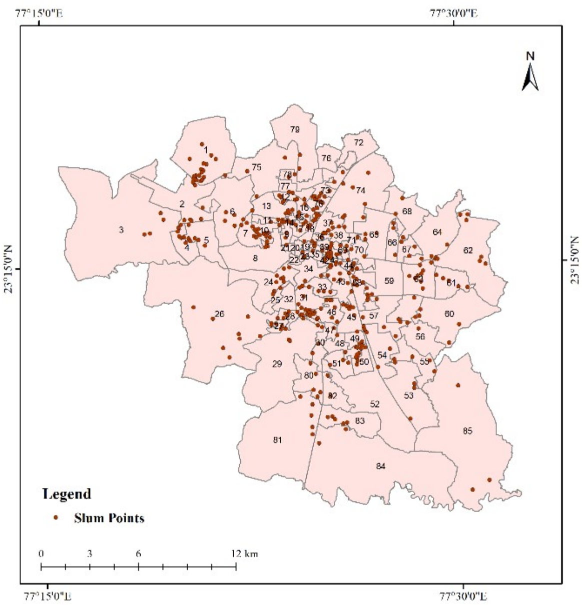

Figure 4. Distribution of Slums

3. METHODOLOGY

The steps followed in the study are outlined in **Figure 5**. The biophysical indicators for the area were obtained using the equations shown below, using ESRI's ArcGIS software.

The most commonly used vegetation index is the normalised difference vegetation index (NDVI) to observe the greenery globally. Healthy plants have a very high reflectance in Near Infrared (NIR). High reflectance in NIR (0.7 to 1.3 µm) and high absorption in Red spectrum, these two bands are used in the following formula to calculate NDVI (Ozyavuz, Bilgili and Salici, 2015). The NDVI value ranges from -1 to 1. High value of NDVI means high reflectance in NIR, implying dense greenery.

$$NDVI = (NIR - Red) / (NIR + Red) \tag{1}$$

Built-up areas and barren land show a drastic increment in their reflectance from NIR to Shortwave Infrared (SWIR) band. Hence, the following formula is used to calculate NDBI (Zha, Gao and Ni, 2003).

$$NDBI = (SWIR - NIR) / (SWIR + NIR) \tag{2}$$

Similarly, water bodies show a good reflectance in Green and a high absorption in SWIR bands. Whereas, built-up areas have high reflectance in SWIR than in Green band. Therefore, the equation below is used for calculating MNDWI (He et al., 2010).

$$MNDWI = (Green - SWIR) / (Green + SWIR) \tag{3}$$

The Land Surface Temperature (LST) is the radiative temperature which is calculated using Top of atmosphere brightness temperature, Wavelength of emitted radiance, Land Surface Emissivity (Anandababu, Purushothaman and Suresh Babu, 2018).

$$LST = (BT / 1) + W * (BT / 14380) * \ln(E) \tag{4}$$

Where BT is Top of atmosphere brightness temperature (°C), W is Wavelength of emitted radiance and E is Land Surface Emissivity.

Normalized difference impervious surface index (NDISI) is used for estimating the impervious surface percentage in an area. Soil, sand, and water generally have a higher reflectance than impervious materials in visible (VIS) bands, and soil and sand have stronger reflectance than impervious materials in middle infrared (MIR) band (Figure 1). Accordingly, the VIS and MIR bands, together with the NIR band, can form a weak-reflectance group of impervious surface (Xu, 2010), hence the following formula is used to compute the index.

$$NDISI = \frac{\left[TIR - \frac{VIS+NIR+SWIR}{3}\right]}{\left[TIR + \frac{VIS+NIR+SWIR}{3}\right]} \tag{5}$$

All the above computed indicators' raster files were overlaid with the ward map of Bhopal. The values were aggregated to the ward level for each of these indicators (raster files) using the spatial analyst functions in GIS.

Socio-economic indicators were extracted from the census data of the BMC. All this data was combined together in the attribute table for different wards if the city. This database was then used in R software as an input for further processing. First, the correlation coefficients between all the indicators were calculated using the Pearson's correlation method. This step is required to examine the relationship between various variables, before we go for the integration of data using Principal Component Analysis (PCA). PCA is a dimension reduction technique. It transforms the data having a large number of correlated variables into a concise data having smaller number of uncorrelated variables. This small number of uncorrelated variables is sufficient to explain most of the variance in the data as compared to too many correlated variables each explaining a very small variance.

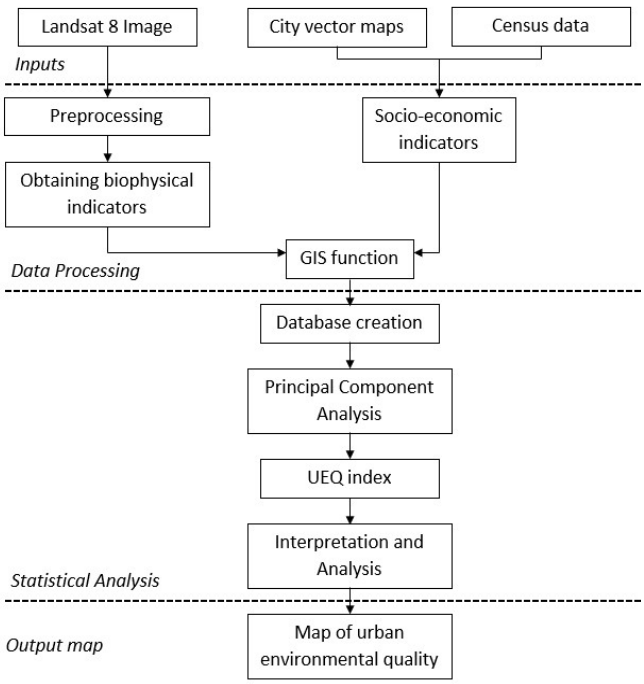

Figure 5. Flowchart representing the procedure to assess the environmental quality.

The first component explains the most variation in the data and the subsequent components explain very little variance. A synthetic index is calculated to describe the environmental quality of each ward which is given below (Musse, Barona and Santana Rodriguez, 2018)

$$UEQI = \sum f_i w_i \quad (6)$$

Where $\sum$ is the summation of '$f_i w_i$' of all the extracted components, f_i be the component score and w_i is the percentage of variance of the i^{th} component.

Ultimately, the component maps were created to represent the variation of each of the components throughout the city. Also, the UEQI maps are generated to represent the environmental quality of each ward. The UEQI values were grouped into five classes enabling the authorities to mark the environmental changes in any ward over time.

4. RESULTS AND DISCUSSION

4.1 Socioeconomic and biophysical indicators

The statistical parameters, i.e., mean and standard deviation of the proposed indicators are presented in **Table 1**.

The PD and HD have higher values mostly in the central region and it fades away as we go the outer periphery of the city.
LST is higher in the regions of high PD and HD and also at some places in the outer regions where there is open barren land.

Table 1. Means, standard deviations, and correlations

Variable	M	SD	1	2	3	4	5	6	7	8	9
1. PD	16548	15333	1								
2. HD	3095	2571	.91**	1							
3. NDVI	0.13	0.04	-.54**	-.57**	1						
4. MNDWI	-0.11	0.04	.12	.11	-.63**	1					
5. NDBI	-0.02	0.02	.49**	.52**	-.46**	-.39**	1				
6. UI	-0.10	0.04	.69**	.72**	-.74**	-.02	.91**	1			
7. LST	31.34	1.38	.26*	.28*	.26*	-.80**	.60**	.39**	1		
8. MNDISI	-0.93	0.01	-.14	-.18	-.51**	.90**	-.38**	-.12	-.85**	1	
9. No of Slums	4.53	2.83	-.26*	-.35**	.28**	-.08	-.20	-.27*	-.02	.07	1

Note. M and SD are used to represent mean and standard deviation, respectively. * indicates $p < .05$. ** indicates $p < .01$.

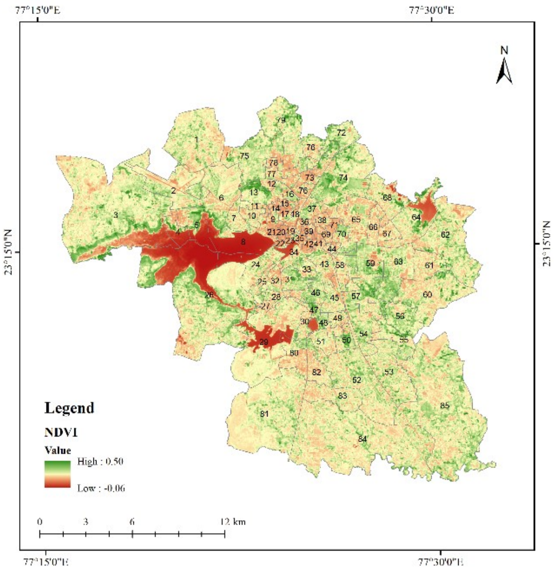

(a)

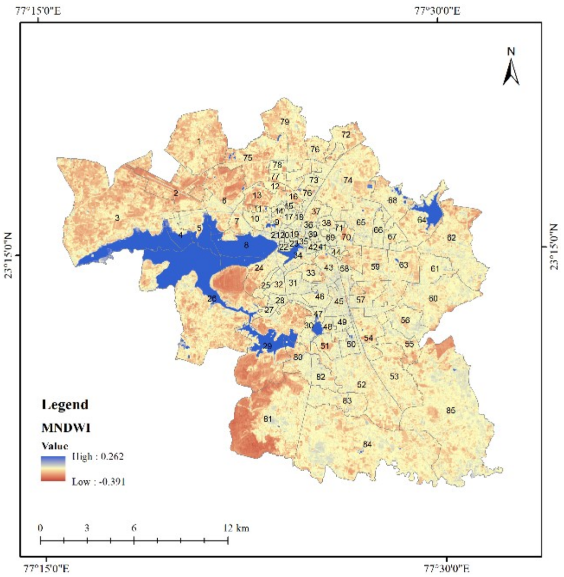

(b)

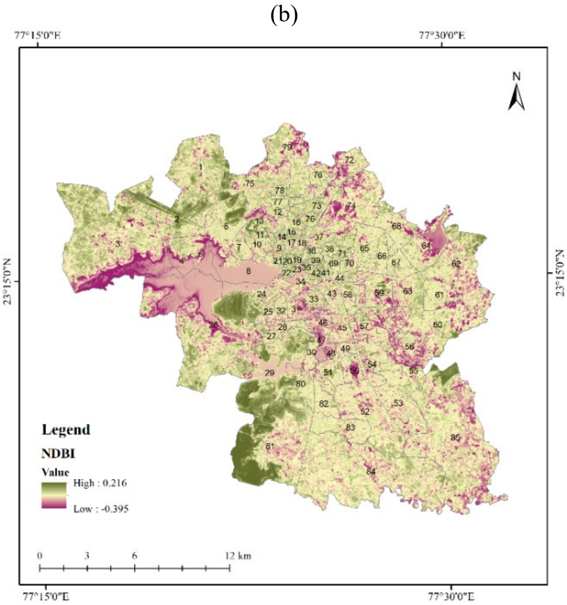

(c)

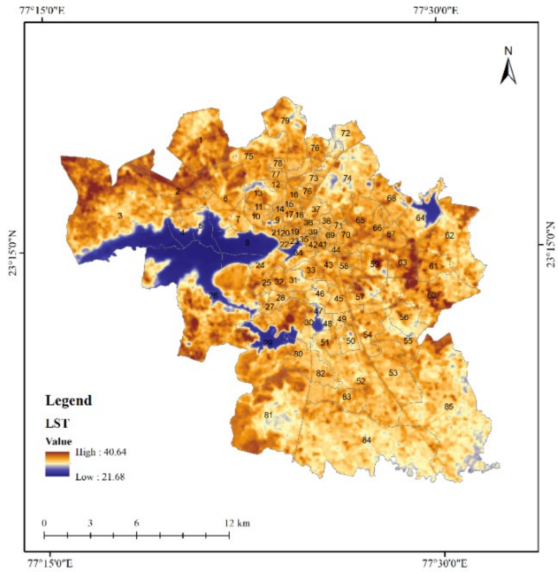

(d)

Figure 6. Images with spatial distribution of (a) NDVI (b) MNDWI (c) NDBI (d) LST

4.2 Statistical Analysis

The data processing section of the methodology involves the database creation at first. For this, the mean values of all the variables for each ward is subjected to Pearson correlation analysis. This is necessary for the application of PCA. The analysis resulted in the correlation matrix as shown in **Table 1**. There is good correlation between NDBI, LST, PD and HD and also between MNDISI and no of slums. A strong negative correlation is seen between LST and MNDWI and also between UI and NDVI. The p-values < .05 and p-values < .01, indicate that there is > 95% and > 99% confidence respectively, that the data is significant and not random. We find that 5 out of 36 correlations (13.8%) and 21 out of 36 correlations (58.33%) were significant at 0.05 and 0.01 level, respectively.

The three principal components (PC) obtained by PCA together show a cumulative variance of 88.61% of the input data. Component loadings in **Table 2** help formulate a relation between the obtained components and input variables.

Table 2. Component scores for the indicators used and the percentage variance

Variables	PC1	PC2	PC3
PD	0.41	0.14	-0.055
HD	0.427	0.138	-0.137
NDVI	-0.285	-0.439	-0.16
MNDWI	-0.967	0.546	-0.008
NDBI	0.436	-0.096	0.262
UI	0.467	0.107	0.22
LST	0.282	-0.434	0.063
MNDISI	-0.187	0.501	0.165
No of slums	-0.189	-0.104	0.897
SD	1.9896	1.7643	0.9506
% of Variance	43.99	34.58	10.04
Cumulative %	43.99	78.57	88.61

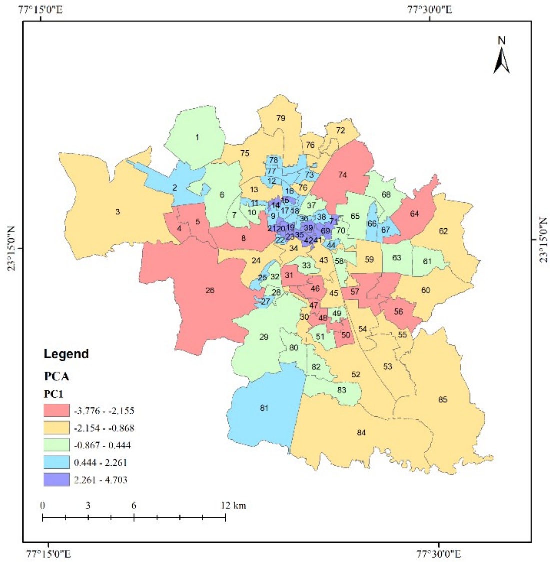

Figure 7. Map of the ward-wise scores of PC1

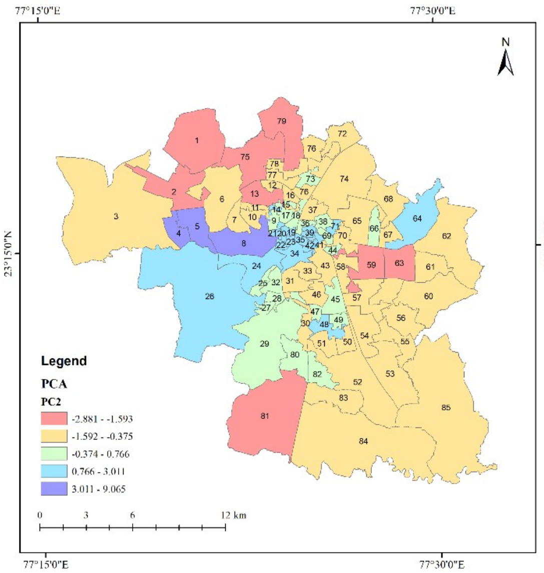

Figure 8. Map of the ward-wise scores of PC2

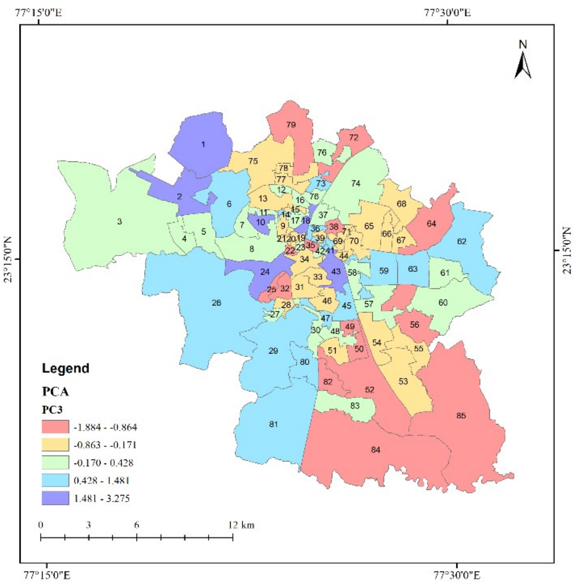

Figure 9. Map of the ward-wise scores of PC3

We see PC1 has a good positive correlation with LST and NDBI, i.e., the variables linked to impervious surfaces (concrete, etc.) and a strong negative correlation with NDVI and MNDWI (vegetation-related indicators). It increases with the increase in impervious surface and decreases with an increase in greenness. It shows the 'adverse effects of land use'. Hence, environmental quality is negatively affected by the score of PC1.

Component 2 has good positive correlation with housing density and population density. It represents overpopulation in the area and termed 'adverse effects of urban design'. The greater the score for PC2, the poorer is the quality of environment.

Component 3 has a strong positive correlation with the no of slums in the individual wards. Higher the number of slums, higher is the score of PC3, poorer is the environmental quality.

Figure 7, **Figure 8**, **Figure 9** show the spatial variation of the three principal components.

4.3 Urban Environmental Quality Index

The scores of the three components are used to calculate the environmental quality index (UEQI). Components 1 and 2 contribute negatively to the environmental quality, hence their scores are reversed (multiplied by -1). Component 3 contributes positively.

$$UEQI = ((43.99 * PC1 * (-1)) + (34.58 * PC2 * (-1)) + (10.04 * PC3 * (-1))) / 100$$

Based on these scores for each ward, the classification was done into 5 categories to explain the environmental quality: very poor, poor, moderate, good and very good.

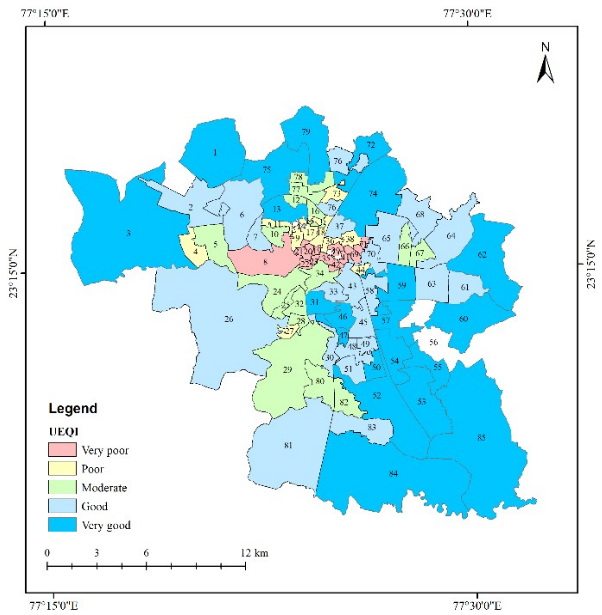

Figure 10. Map of ward-wise urban environmental quality of Bhopal

Figure 10 shows the spatial distribution of UEQI and indicates that the overall environmental quality of Bhopal is very moderate. The wards with poor UEQI value are mostly towards the centre of the city (wards 4, 8, 9, 11, 15, 17-23, 27, 35-39,

https://doi.org/10.5194/isprs-archives-XLIII-B3-2022-705-2022 |

42, 44, 69, 73, 77-78). These are very densely populated areas. On the contrary, the wards with good environmental quality are in the sparsely populated areas that lie near the edges of the city. These are the areas with good plantation and lower temperatures with small water bodies in between (3, 5, 13, 26, 30, 46-48, 50, 52-57, 59, 63, 64, 72, 74, 75, 79, 81, 83-85).

5. CONCLUSION

In the study, various indicators to be used for environmental quality assessment are identified for Bhopal city. The model and procedure used here can be applied to any other city as well.
Since, environmental quality is a multi-disciplinary subject, there does not exist any standard procedure or technique to assess it. The approach used in this study interprets the relationship between various indicators used.

The results depicted that the highest value of our developed index occurred in the places where there is more greenery and less built-up area. The index values suggest that urban greening significantly contributes to enhancing the urban environmental quality. Also, it highlights the critical zones where intervention should be done by the planners and policymakers for the sustainability of the city. Periodic calculation of UEQI enables monitoring the effect of developments spatially and periodically.

Although, even more variables can be used that were not accounted in the study, such as the economic status, air quality, noise levels, etc. of different localities, which is a scope for further research.

REFERENCES

Anandababu, D., Purushothaman, B. M. and Suresh Babu, S. (2018) 'Estimation of Land Surface Temperature using LANDSAT 8 Data', International Journal of Advance Research, 4(2), pp. 177–186. Available at: www.IJARIIT.com.

Chudnovsky, A., Ben-Dor, E. and Saaroni, H. (2004) 'Diurnal thermal behavior of selected urban objects using remote sensing measurements', Energy and Buildings, 36(11), pp. 1063–1074. doi: 10.1016/J.ENBUILD.2004.01.052.

Cui, L. and Shi, J. (2012) 'Urbanization and its environmental effects in Shanghai, China', Urban Climate, 2, pp. 1–15. doi: 10.1016/J.UCLIM.2012.10.008.

Dawson, R. et al. (2017) 'A blueprint for the integrated assessment of climate change in cities', Green CITYnomics: The Urban War against Climate Change, pp. 32–51. doi: 10.4324/9781351279444-3/BLUEPRINT-INTEGRATED-ASSESSMENT-CLIMATE-CHANGE-CITIES-RICHARD-DAWSON-JIM-HALL-STUART-BARR-MIKE-BATTY-ABIGAIL-BRISTOW-SEBASTIAN-CARNEY-ATHANASIOS-DAGOUMAS-STEPHEN-EVANS-ALISTAIR-FORD-HELEN-HARWATT-JONATHAN-K.

Du, P. et al. (2014) 'Remote sensing image interpretation for urban environment analysis: Methods, system and examples', Remote Sensing, 6(10), pp. 9458–9474. doi: 10.3390/rs6109458.

He, C. et al. (2010) 'Improving the normalized difference built-up index to map urban built-up areas using a semiautomatic segmentation approach', Remote Sensing Letters, 1(4), pp. 213–221. doi: 10.1080/01431161.2010.481681.

Musse, M. A., Barona, D. A. and Santana Rodriguez, L. M. (2018) 'Urban environmental quality assessment using remote sensing and census data', International Journal of Applied Earth Observation and Geoinformation, 71(May), pp. 95–108. doi: 10.1016/j.jag.2018.05.010.

Nichol, J. and Wong, M. S. (2005) 'Modeling urban environmental quality in a tropical city', Landscape and Urban Planning, 73(1), pp. 49–58. doi: 10.1016/j.landurbplan.2004.08.004.

Nong, Y. and Du, Q. (2011) 'Urban growth pattern modeling using logistic regression', Geo-Spatial Information Science, 14(1), pp. 62–67. doi: 10.1007/S11806-011-0427-X.

Ozyavuz, M., Bilgili, B. C. and Salici, A. (2015) 'Determination of vegetation changes with NDVI method', Journal of Environmental Protection and Ecology, 16(1), pp. 264–273.

Silva, E. A. and Clarke, K. C. (2002) 'Calibration of the SLEUTH urban growth model for Lisbon and Porto, Portugal', Computers, Environment and Urban Systems, 26(6), pp. 525–552. doi: 10.1016/S0198-9715(01)00014-X.

Verma, P. and Raghubanshi, A. S. (2018) 'Urban sustainability indicators: Challenges and opportunities', Ecological Indicators, 93(May), pp. 282–291. doi: 10.1016/j.ecolind.2018.05.007.

Xu, H. (2010) 'Analysis of impervious surface and its impact on Urban heat environment using the normalized difference impervious surface index (NDISI)', Photogrammetric Engineering and Remote Sensing, 76(5), pp. 557–565. doi: 10.14358/PERS.76.5.557.

Zha, Y., Gao, J. and Ni, S. (2003) 'Use of normalized difference built-up index in automatically mapping urban areas from TM imagery', International Journal of Remote Sensing, 24(3), pp. 583–594. doi: 10.1080/01431160304987.